

Large Area Propellers

Daniel Knutsson¹, Lars Larsson²

¹ PhD student, Department of Shipping and Marine Technology, Chalmers University of Technology, Gothenburg, Sweden

² Professor of Hydrodynamics, Department of Shipping and Marine Technology, Chalmers University of Technology, Gothenburg, Sweden

ABSTRACT

The high cost of fuel and the demanding regulations against the environmental impact of using fossil fuels are now encouraging new and more radical solutions when it comes to the propulsion systems of a ship. One possible way is to move the propeller aft behind the hull. This allows the propeller diameter to increase without risks of pressure pulses being transferred to the hull. An increase in efficiency may then be achieved, reducing environmental impacts and cost. This is referred to as the large area propeller (LAP) concept and is investigated in this paper. The CFD software SHIPFLOW with a zonal approach (RANS, potential flow and boundary layer methods) is used, and the propeller is represented by a lifting line method. The original propeller and a larger one are systematically moved aft, and the delivered power, as well as the propulsive coefficients, are computed. Results are compared with experimental data from SSPA. The results indicate a large reduction in delivered power both in CFD and EFD by moving the propeller aft and increasing the diameter by 22.7%. Compared to the original configuration, the reduction is around 10% in EFD and 14% in CFD; however, the trends are well captured in CFD. There is thus a large gain in total efficiency mainly due to increased hull and propeller efficiencies, even though no modifications of the hull and propellers were done to further improve the concept. By optimizing these, it could be possible to improve the concept even further.

1 INTRODUCTION

In order to meet the environmental challenges on the marine transport industry over the next 25 years, as predicted by the World Bank (Streamline 2008), the vessels and propulsion systems need to be more efficient. Less conservative solutions may be necessary to meet this requirement. It has been known for a long time that an increase in propeller diameter will result in increased propulsive efficiency. In this paper, the total propulsive efficiency will be broken down into components to distinguish the different effects. This work is a part of a larger investigation, aiming at detecting suitable hull types for a LAP concept. The starting point of this investigation is to do systematic variations of propellers with different diameters and

longitudinal positions for a given state-of-the-art preliminary design. A second step will be to repeat the systematic variation for other hull types suitable for LAP and look for general trends (if any), and to select the most promising hull for further improvements using optimization tools. The hulls and propellers used throughout this project are carefully chosen with guidance from SSPA and Rolls Royce.

2 TEST CASE

The systematic variations were carried out for a small single screw tanker (8000ton) designed by Rolls Royce in Norway. Two propellers were used, the original one (OP) and one larger propeller referred to as the LAP. The propellers were carefully chosen to match the design conditions of the tanker. Both propellers were systematically moved back in seven steps, from the original position to a position located far behind transom stern. The hull and propeller data are given in Table 1 and Table 2.

MODEL HULL DATA	
Length L_{WL} [m]	5.59
Beam B_{WL} [m]	0.908
Trim t [deg]	0
Draft T_{FP}, T_{AP} [m]	0.344
Displacement ∇ [m ³]	1.26
Block coefficient C_B	0.7443
Wetted surface S_S [m ²]	7.38
Wetted surface $T_{transom}$ [m ³]	0.014
Scale α [-]	1:20.909

Table 1: Hull data

Large area propeller (LAP)	
Propeller diameter [mm]	270
Chord length $R_{0.75}$ [mm]	60
Number of blades Z	4
Max thickness $R_{0.75}$ [mm]	3.34
Pitch ratio at $R_{0.75}$ [-]	0.823
Scale- α [-]	1:20.909
Original propeller (OP)	
Propeller diameter [mm]	220
Chord length $R_{0.75}$ [mm]	89
Number of blades Z	4
Max thickness $R_{0.75}$ [mm]	3.4
Pitch ratio at $R_{0.75}$ [-]	0.866
Scale- α [-]	1:20.909

Table 2: Propeller data

The design speed at model scale for the tanker is 1.63 m/s, which corresponds to a Froude number of 0.22. A Froude number of this magnitude is considered high for traditional tankers; however, for this more slender tanker it is not a problem. Rendering pictures can be seen in Figures 1 and 2.

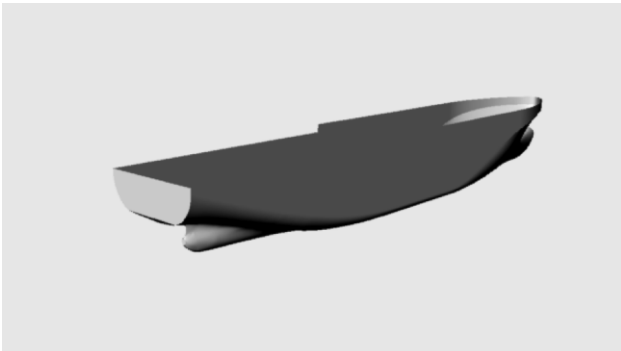


Figure 1: Tanker, side view from stern

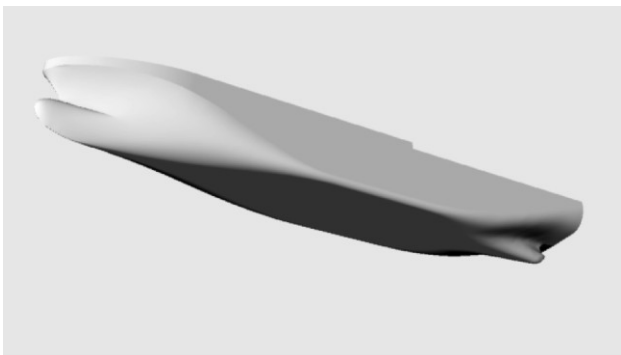


Figure 2: Tanker, side view from bow

2.1 Validation test at SSPA

One bare hull resistance test and three self-propulsion tests were carried out at SSPA to validate the CFD computations. One of the positions was determined from CFD to be the optimum position and one was the original configuration. Two self-propulsion tests were done at the optimum positions, one with the LAP and one with the original propeller. The remaining test was in original position with the original propeller and this was used as a benchmark. The model scale tests were identical to the CFD simulations and the dimensions are seen in Table 1 and Table 2. All tests, both in EFD and CFD, were made without a rudder.

3 METHODS

The simulations were done using the software SHIPFLOW, Version 4.4. This software is specialized for naval applications. The simulation in this case was based on a zonal approach (Regnström 2010), in which different zones use different methods to resolve the flow, as illustrated in Figure 3.

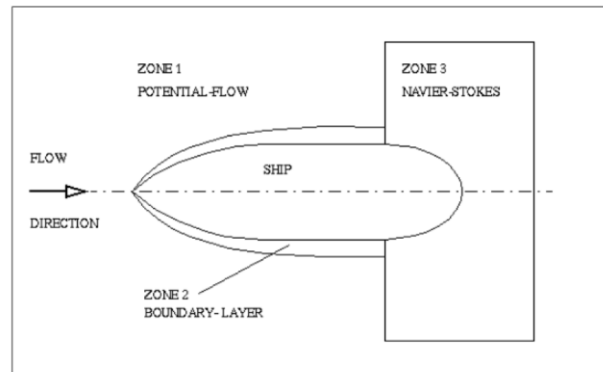


Figure 3: Zonal approach

3.1 Zone 1

The potential flow solver is used for computing the wave pattern, wave resistance, trim and sinkage in this case. The potential flow method also provides necessary input to the boundary layer method.

3.2 Zone 2

A simple boundary layer method is used to compute the viscous resistance in the fore part of the hull, where the boundary layer is thin. The boundary layer method also provides the necessary input to the RANS solver for the aft part.

3.3 Zone 3

A Reynolds-averaged Navier-Stokes (RANS) method is used to resolve the thicker boundary layer and wake field using a $k-\omega$ SST turbulence model (Regnström 2007). The wavy surface is imported from potential flow and the RANS grid is fitted to this surface. This is done to have a more accurate representation of the flow without sacrificing computation cost. An illustration of

the wavy surface in the RANS grid is shown in Figure 4.

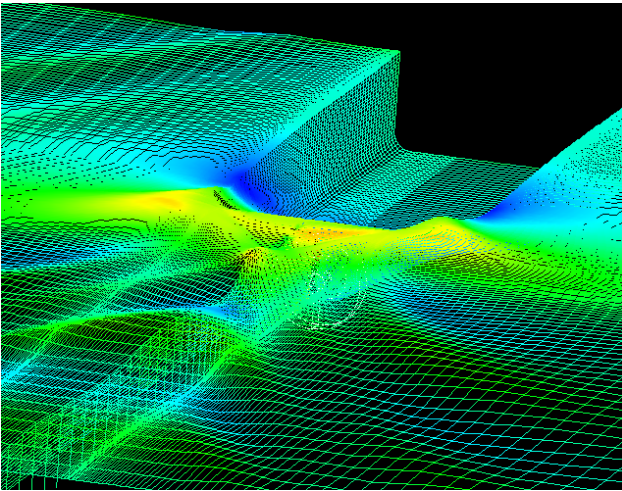


Figure 4: Wavy surface and RANS grid

3.4 Lifting Line (LL)

The propeller is represented by a lifting line method. In this method, the lift and drag are obtained from 2-D wing theory for a number of blade sections, and integration along the span gives the torque and thrust (Dyne 1967). The result depends on the local flow and blade geometry such as: camber ratio, pitch ratio, blade thickness and chord length.

The interactive coupling between the RANS solver and the LL method is achieved through body forces accelerating the flow (Han 2008). The induced velocity from the propeller is subtracted from RANS every tenth iteration to get the effective wake distribution for next LL iteration. Axial and tangential forces are computed and distributed over the volume cells in the propeller grid. The forces will give the fluid passing through a longitudinal and angular momentum, consistent with the thrust and torque of the propeller.

3.5 Resistance and force balancing

The resistance and thrust are balanced for a given speed by adjusting the rate of revolution of the propeller (equivalent to a self-propulsion test). Since this is done at model scale, a towing force R_a has to be applied to correctly scale the loading of the propeller.

The total bare hull resistance is more accurate if the different resistance components are calculated separately. Using the wavy surface in RANS should, in principle, give the total resistance (neglecting the fact that the boundary conditions for the viscous flow are not exactly satisfied on the pre-computed surface), but since there were waves only in zone 3 the resistance cannot be computed in this way. However, the flow into the propeller is better captured with a wavy surface, so this was used throughout the simulations. It should be noted that the influence of the propeller on the waves is neglected in this approach.

3.6 Open water simulations

Open water characteristics were also calculated using RANS and LL. This was necessary to obtain the relative rotative efficiency, but also to compare the results with experimental data to see if the propeller is represented well using LL.

4 RESULTS

In this section, we will first give the results of the validation. The computed thrust and delivered power will be compared with the data measured at SSPA. Thereafter, the results of the systematic computations will be presented and analyzed. This is done for 7 positions using both propellers, from position 0 (original position) to position 6 (aftmost position). Position number 2 is the one chosen for the tests, “the optimum”, and is located just behind the transom stern. The reason is high efficiency and clearance for the LAP. The different positions in meters using the original position as reference are: 0, 0.137, 0.201, 0.264, 0.391, 0.518, 0.645, respectively, as shown in Figure 5.

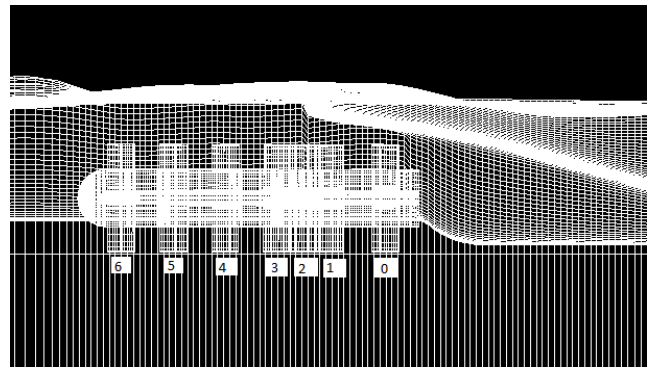


Figure 5: Propeller positions from pos0-pos6; Pos6 is the aft most one

4.1 Validation

Results of the validation are shown in Table 3. The thrust, T , and delivered power, PD , are given for all three tested conditions: the original propeller, OP in the original position 0, and OP and LAP at the optimum position 2. The differences, dT and dPD between SHIPFLOW and the SSPA data are also given in percent of the data. Finally, the predicted and measured gain at position 2 for the two propellers, compared to the original configuration, is presented.

As seen in the table, there is generally a very good correspondence between computations and measurements. The thrust difference is within a couple of percentage points for all cases and the power difference is within a fraction of a percent for the original propeller. For the LAP, the difference is larger however. This means that the gain in power is very accurately predicted for the OP (7.3% compared with 7.0%), while it is overpredicted for the LAP (14.4% compared with 9.8%). In spite of this, the validation must be considered satisfactory.

SHIPFLOW VS SSPA							
		T [N]	PD [W]	Deviation T	Deviation PD	Gain SF	Gain SSPA
SP0	SHIPFLOW	38.6	78.4	1.45%	0.10%	0.00%	0.00%
	SSPA	39.2	78.5				
SP2	SHIPFLOW	35.9	72.7	2.33%	0.42%	7.26%	6.96%
	SSPA	35.0	73.0				
LP2	SHIPFLOW	36.1	67.1	1.20%	5.13%	14.35%	9.82%
	SSPA	36.5	70.7				

Table 3: Thrust and delivered power from CFD and EFD; two positions (0, 2) and two propellers (OP and LAP)

4.2 Wake fraction and thrust deduction

As seen in Figure 6, the thrust deduction factor, t , drops rapidly in the first step when moving the propeller backwards from its original position. The development of t versus distance is very similar for both propellers.

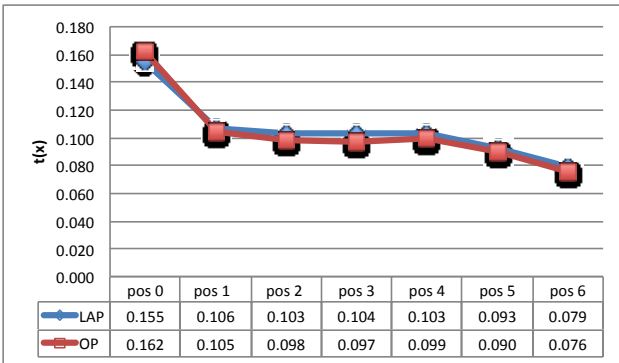


Figure 6: Variation of t with propeller position. LAP vs OP

The wake fraction, w_{tm} , also exhibits the largest drop at the first step, as seen in Figure 7. However, the drop is not as large as for t .

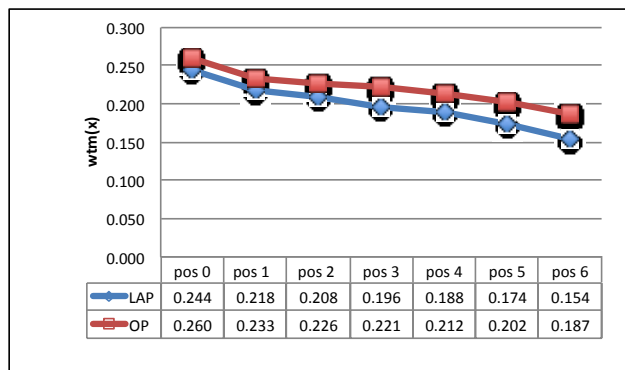


Figure 7: Variation of w_{tm} with propeller position; LAP vs OP

In Figure 7, the values for the LAP are significantly smaller than for the original propeller. This is easily explained since the LAP operates further out in the boundary layer representing the wake behind the hull.

When combining these factors to determine the hull efficiency, it is noticed that efficiency has a global maximum at position 1 for both propellers. The original propeller has higher hull efficiency over the whole span, explained by w_{tm} . This is illustrated in Figure 8.

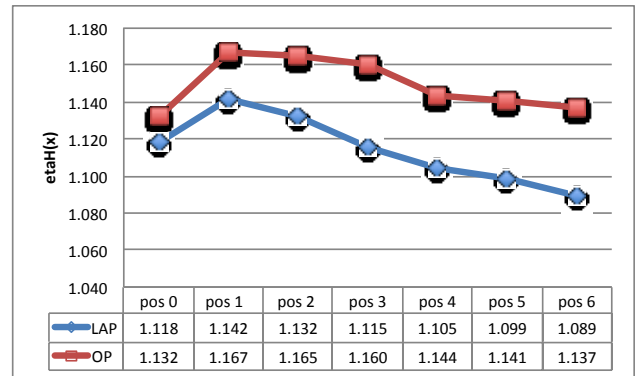


Figure 8: Variation of hull efficiency with propeller position; LAP vs OP

To illustrate the physics behind the development of the hull efficiency, the axial velocity at a cut just in front of the propeller is presented for three different positions of the LAP. The first position is the original one, the second is the tested position 2, and the third is the aftmost position (pos 6). The pressure distribution on the aft part of the hull is also given in Figures 9, 10 and 11.

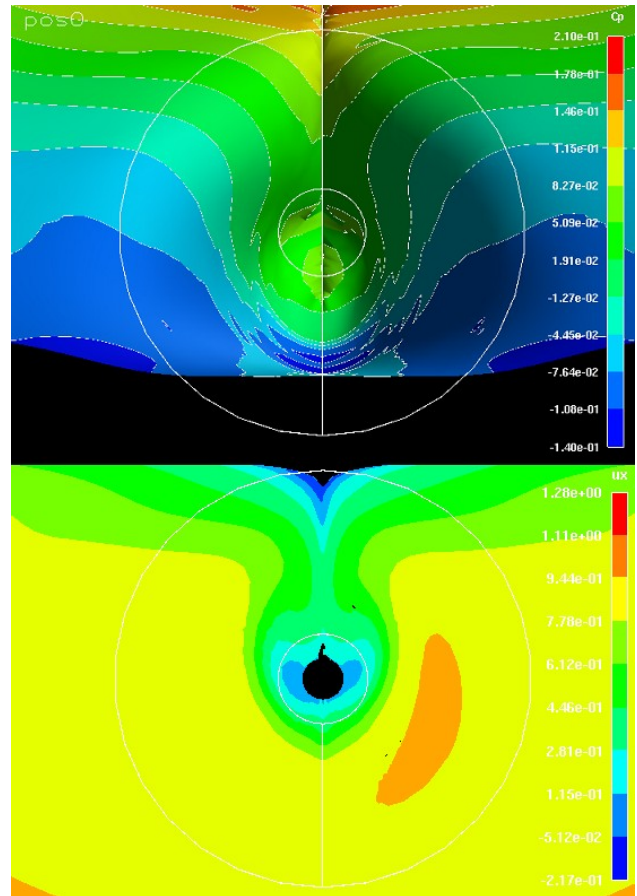


Figure 9: Pressure distribution on hull and total velocity just upstream the propeller for pos0 with LAP

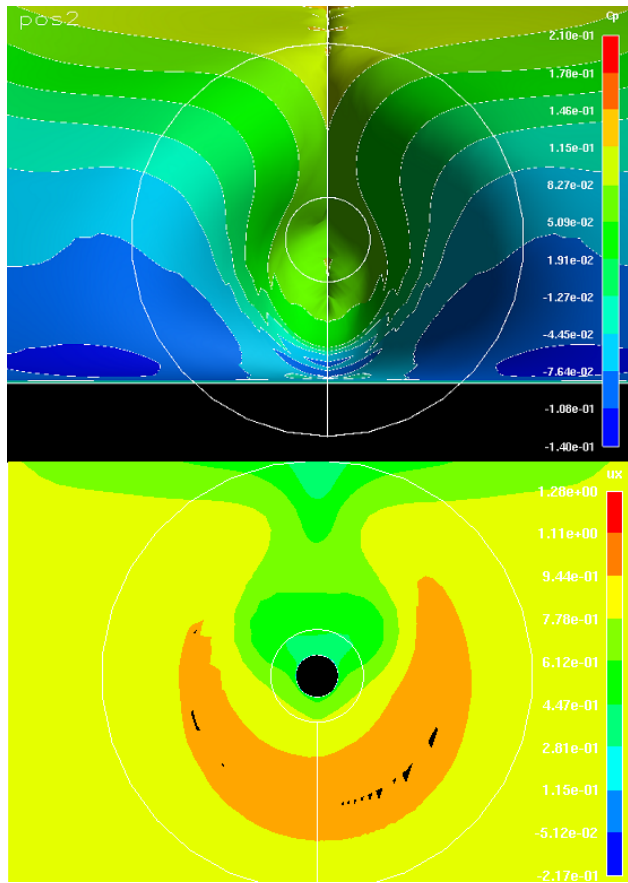


Figure 10: Pressure distribution on hull and axial velocity just upstream the propeller for pos2 with LAP

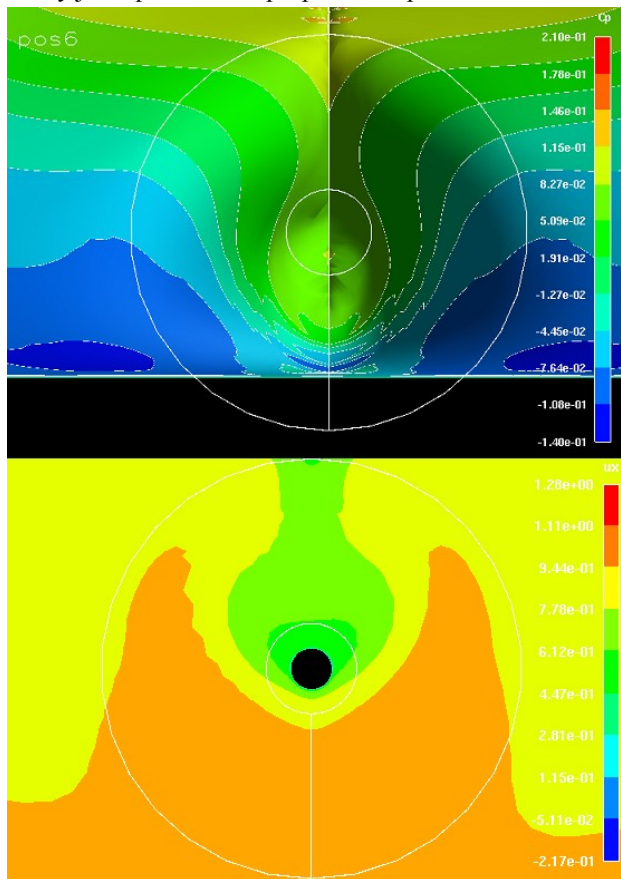


Figure 11: Pressure distribution on hull and axial velocity just upstream the propeller for pos6 with LAP

As seen from figures 9-11, the pressure on the hull increases when moving the propeller aft. When a propeller operates close to the hull, it increases the flow velocity in front of the propeller disk and thereby reduces the pressure on the hull surface. This is the main cause of the thrust deduction, but there is also a contribution from the increased friction. The velocity distribution is seen in the lower part of the figures. As expected, the velocity is increased and the propeller operates closer to the free stream velocity when moving the propeller aft.

4.3 Relative rotative efficiency

The relative rotative efficiency of the propeller also shows some interesting trends. The efficiency, shown in Figure 12, is highest for the original position and other positions close to the hull, where the wake still is strongly inhomogeneous. It decreases with distance from hull and becomes closer to unity for the aftmost position. There may be several reasons for this. In the uneven wake flow the drag of the propeller sections is reduced due to the Katzmayr effect (Katzmayr 1922), which results in a reduction of K_Q for a given K_T . Another reason is that the propellers is wake adapted, i.e., designed for the hull wake. They may thus be assumed less efficient in a homogenous inflow. It could also be noticed that the relative rotative efficiency is higher for LAP in general (around 1-2% higher), which was also indicated in measurements.

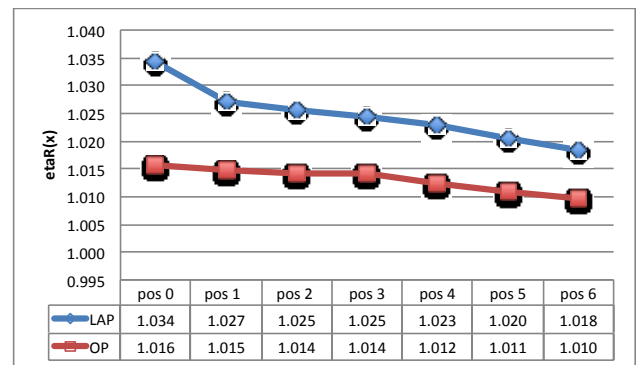


Figure 12: Variation of relative rotative efficiency with propeller position; LAP vs OP

4.4 Open water efficiency

The open water curves shows a very good agreement using LL compared to experimental data, especially for advance ratios between 0.45-0.8, as can be seen in Figures 13 and 14. The difference is only around 1-2% depending on advance ratio and propeller.

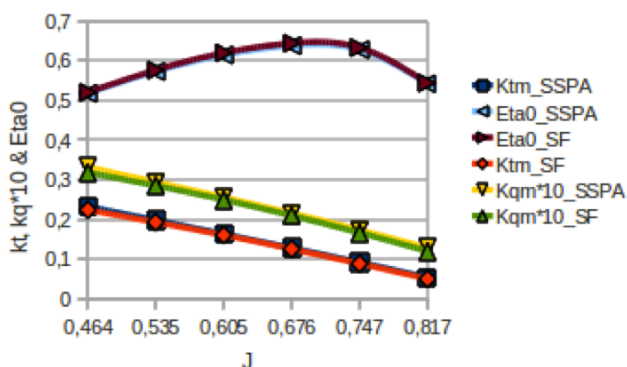


Figure 13: Comparing open water results for the original propeller using LL and experimental data (SF: SHIPFLOW)

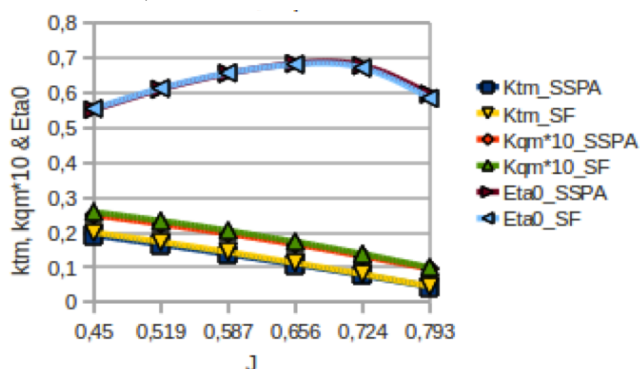


Figure 14: Comparing open water results for LAP using LL and experimental data

The propeller efficiency is shown for both propellers and all positions in Figure 15. LAP shows a significantly larger efficiency and this really shows the main reason for using this type of concept. Note that both propellers operate close to optimum working point.

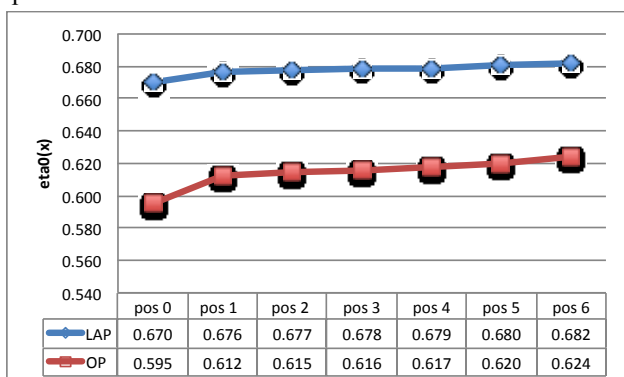


Figure 15: Variation of propeller efficiency with propeller position; LAP vs OP

4.5 Delivered power

Having analyzed all contributions to the final efficiency, Figures 16 and 17 show the variation of the total efficiency and delivered power with position. The minimum delivered power is obtained at pos2 for the original propeller and pos1 for the LAP. The reason for the better total efficiency at pos2 of the original propeller is the open water efficiency, which increases

more than the decrease in relative rotative and hull efficiency when moving from pos1 to pos2. While pos1 is best for the LAP, the difference is very small compared to pos2 and there are other benefits of having the propeller located just behind the hull. The primary reason is larger clearance and less pressure pulses. It is also possible to increase the diameter even more using pos2. The figures show better total efficiency (and thus less power) for all positions using LAP compared to the original propeller.

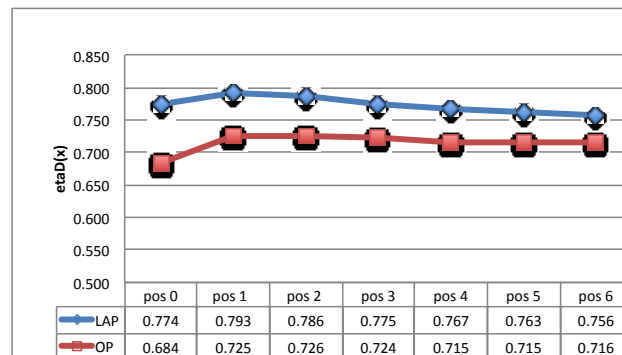


Figure 16: Variation of total propulsive efficiency with propeller position; LAP vs OP

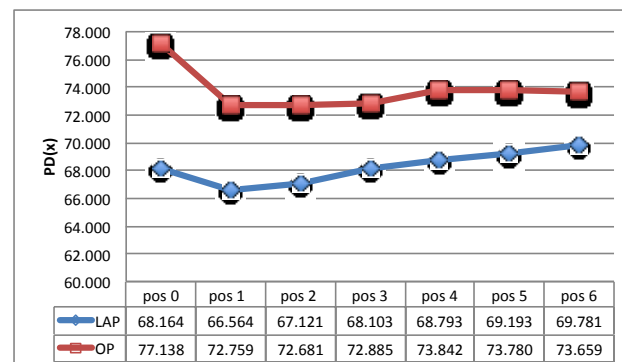


Figure 17: Variation of delivered power with propeller position; LAP vs OP

5 CONCLUSIONS

Moving the propeller aft and increasing the area indicated a great potential for power reduction. Interesting trends in propulsive factors were revealed in the simulations and verified in experiments. Since the investigation was carried out without rudder and without optimizations of hull and propellers, there is room for further improvements to reduce power. Further simulations should include the neglected effect of the propeller on the free surface. Wave elevation changes as well as air suction should then be considered.

ACKNOWLEDGEMENTS

The authors are indebted to Rolls-Royce AB and SSPA AB for support and guidance throughout the project, and for providing necessary data. Special thanks are due to Mr. Jan-Olov Forsström who proposed the basic idea behind the LAP concept.

The staff at FLOWTECH International AB is also acknowledged for support in the use of the SHIPFLOW code. The research presented in this paper has received funding from the European Union Seventh Framework Programme (FP7/2007- 2013) under grant agreement n°233896.

REFERENCES

Regnström, B (2010). SHIPFLOW manual. FLOWTECH International AB.

Han, K-J. (2008). Numerical optimization of hull/propeller/rudder configurations. PhD Thesis, Department of Shipping and Marine Technology, Chalmers University of Technology, Sweden.

Dyne, G. (1967). 'A method for the design of ducted propellers in uniform flow'. SSPA Publications Report 62, Gothenburg, Sweden.

Streamline. (2008). 'Strategic Research for innovative Marine propulsion concepts'. Streamline, Rolls Royce 1.1.6.

Regnström, B. (2007). XCHAP theoretical manual. FLOWTECH International AB.

Katzmayr, R. (1922). 'Effect of periodic changes of angle of attack on behavior of airfoils'. NACA Technical Report TM 147.